SCIENTIFIC REPORTS

OPEN

SUBJECT AREAS:
SUPERCONDUCTING PROPERTIES AND MATERIALS
ELECTRONIC PROPERTIES AND MATERIALS
BOSE-EINSTEIN CONDENSATES

Received
30 August 2013

Accepted
30 January 2014

Published
28 February 2014

Correspondence and requests for materials should be addressed to K.O. (okazaki@wyvern.phys.s.u-tokyo.ac.jp) or S.S. (shin@issp.u-tokyo.ac.jp)

* Current address: Department of Physics, University of Tokyo, Tokyo 113-0033, Japan.

† Current address: Japan Synchrotron Radiation Research Institute (JASRI/SPring-8), Sayo, Hyogo 679-5198, Japan.

‡ Current address: Department of Applied Physics, University of Tokyo, Tokyo 113-8656, Japan.

§ Current address: Graduate School of Engineering Science, Osaka University, Osaka 560-8531, Japan.

Superconductivity in an electron band just above the Fermi level: possible route to BCS-BEC superconductivity

K. Okazaki[1]*, Y. Ito[1], Y. Ota[1], Y. Kotani[1]†, T. Shimojima[1]‡, T. Kiss[1]§, S. Watanabe[2], C.-T. Chen[3], S. Niitaka[4,5], T. Hanaguri[4,5], H. Takagi[4,5], A. Chainani[6,7] & S. Shin[1,5,6,8]

[1]Institute for Solid State Physics (ISSP), University of Tokyo, Kashiwa, Chiba 277-8581, Japan, [2]Research Institute for Science and Technology, Tokyo University of Science, Chiba 278-8510, Japan, [3]Beijing Center for Crystal R&D, Chinese Academy of Science (CAS), Zhongguancun, Beijing 100190, China, [4]RIKEN Advanced Science Institute, 2-1, Hirosawa, Wako, Saitama 351-0198, Japan, [5]TRIP, JST, Chiyoda-ku, Tokyo 102-0075, Japan, [6]RIKEN SPring-8 Center, Sayo-gun, Hyogo 679-5148, Japan, [7]Department of Physics, Tohoku University, Aramaki, Aoba-ku, Sendai 980-8578 Japan, [8]CREST, JST, Chiyoda-ku, Tokyo 102-0075, Japan.

Conventional superconductivity follows Bardeen-Cooper-Schrieffer(BCS) theory of electrons-pairing in momentum-space, while superfluidity is the Bose-Einstein condensation(BEC) of atoms paired in real-space. These properties of solid metals and ultra-cold gases, respectively, are connected by the BCS-BEC crossover. Here we investigate the band dispersions in $FeTe_{0.6}Se_{0.4}$($T_c = 14.5$ K ~ 1.2 meV) in an accessible range below and above the Fermi level(E_F) using ultra-high resolution laser angle-resolved photoemission spectroscopy. We uncover an electron band lying just 0.7 meV ($\sim$8 K) above E_F at the Γ-point, which shows a sharp superconducting coherence peak with gap formation below T_c. The estimated superconducting gap Δ and Fermi energy ϵ_F indicate composite superconductivity in an iron-based superconductor, consisting of strong-coupling BEC in the electron band and weak-coupling BCS-like superconductivity in the hole band. The study identifies the possible route to BCS-BEC superconductivity.

The iron-based high-temperature superconductors[1] possess multi-band hole and electron Fermi surfaces (FSs) which have motivated the role of FS nesting, spin- and orbital-fluctuations, or a combination of these mechanisms for understanding their properties[2–4]. Electronic structure studies have concentrated on band dispersions in the occupied states lying below the Fermi level (E_F)[5–7], which open up a superconducting gap (Δ) below T_c. However, the observation of a pseudogap in the normal phase of the high-T_c copper oxide superconductors[8,9] identified a remarkable challenge in our understanding of superconductivity and its origin is still extensively debated. In particular, does the pseudogap represent preformed Cooper pairs, or does it reflect another ground state competing with superconductivity[10–12]? More recently, a pseudogap was also found in the strongly interacting ultracold Fermi gas above the superfluid condensation temperature[13]. These fascinating results suggest the important role of pairing in the normal phase, above the onset of superfluidity/superconductivity in strongly interacting systems. The existence of a pseudogap state has been discussed in the scheme of BCS-BEC crossover[14]. Very interestingly, the study on ultracold Fermi gases reported a pseudogap for a system with $\Delta/\epsilon_F \sim 1$[13] while the optimally doped copper oxide Bi2212 shows a $\Delta/\epsilon_F \sim 0.1$[7]. In a recent study on the Fe(Te,Se) superconductor, it was concluded that the system was in the BCS-BEC crossover regime with a $\Delta/\epsilon_F \sim 0.5$ associated with a hole band centered at the Γ-point[7]. The obtained band dispersions were similar to prior studies of the normal phase[15,16], while Δ was much smaller than an earlier report which claimed strong coupling superconductivity[17]. Although a pseudogap is expected based on theories of the BCS-BEC crossover[18–21], no study to date has identified a pseudogap in the momentum resolved electronic structure of Fe(Te,Se). Further, a tuning of the BCS to BEC regimes across the Feshbach resonance using a magnetic field which eventually leads to a change in sign of the chemical potential for fermions[21], is well-known in ultracold atomic gases[22,23]. However, a similar control of the chemical potential in a solid is not possible, and consequently, the BEC superconductivity in a solid has eluded experiments. In the following, we report experiments indicative of composite superconductivity in an iron-based superconductor: Cooper pairing in a hole band coexisting with Bose-Einstein condensation in an electron band.

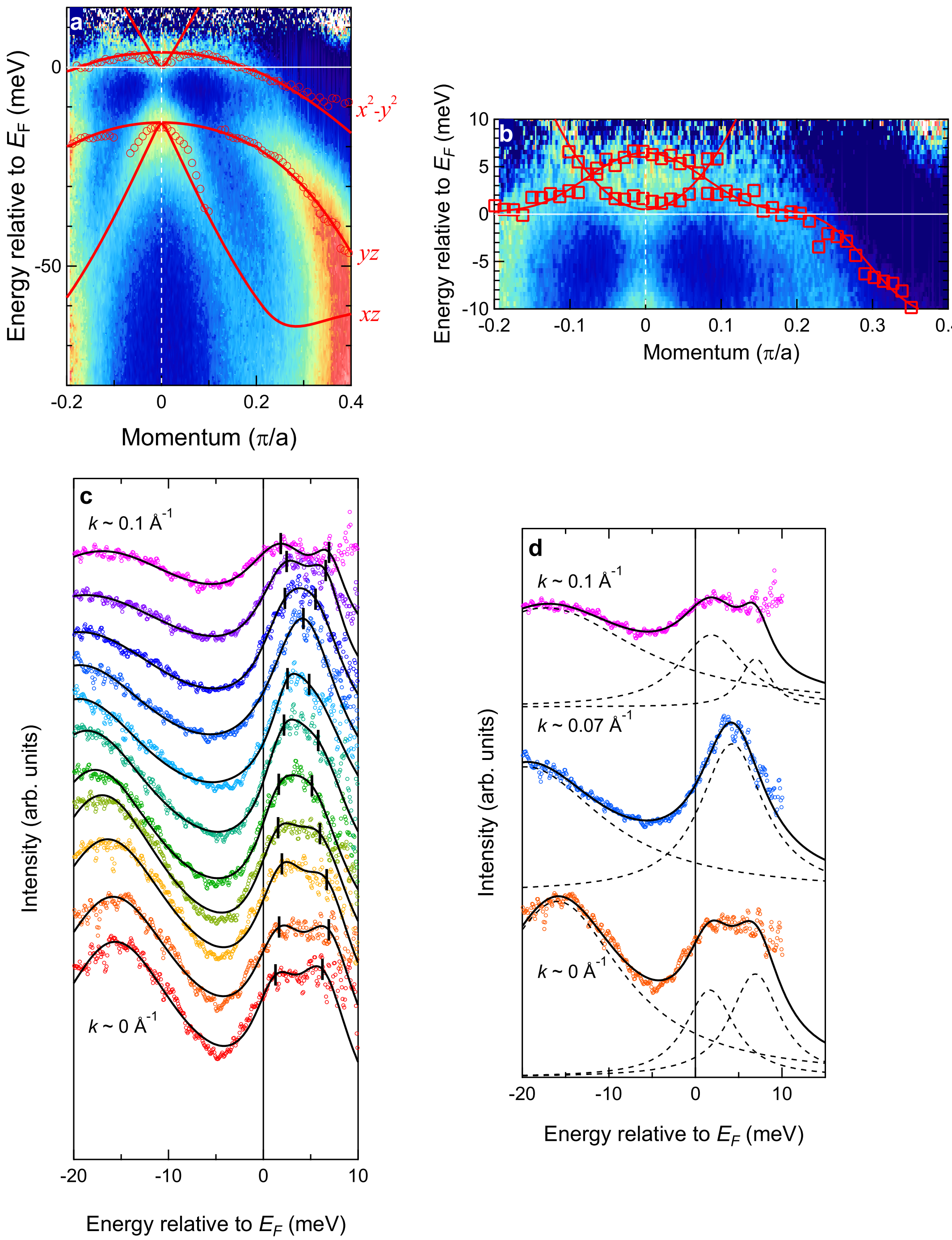

Figure 1 | Band dispersions of $FeTe_{0.6}Se_{0.4}$ along Γ-*X* line measured at 25 K. (a) Intensity plot of *E* vs. *k* measured at 25 K along Γ-*X* line. The shifted and rescaled DFT result is overlaid as solid lines. The open circles indicate band dispersions deduced from the peak positions of the second derivative spectra. (b) Intensity plot near E_F. The open rectangles indicate band dispersions deduced from the fitting to the EDCs. The solid lines are dispersions by fitting to the rectangles with a polynomial function. (c) Fitting to several cuts of EDCs after dividing by the FD function. The solid lines indicate the fitting results. The fitting functions were obtained using three Lorentzians convoluted with the Gaussian corresponding to the experimental energy resolution. (d) Fitting results with the component Lorentzians for three cases, around the Γ point, $k \sim 0.07$ *Å*, and $k \sim 0.1$ *Å*.

Results

Electron band lying just above E_F. Figure 1(a) shows an intensity plot of *E* vs. *k* (energy vs. momentum) measured at 25 K ($>T_c$ = 14.5 K) along Γ-*X* line in the Brillouin zone of $FeTe_{0.6}Se_{0.4}$ after dividing by the Fermi-Dirac (FD) function broadened with the Gaussian corresponding to the experimental energy resolution. We employed three different methods to determine the band dispersions: a second derivative map with respect to energy, fitting to the energy distribution curves (EDCs), and fitting to the momentum distribution curves (MDCs) (see Supplementary Information). Three hole bands can be clearly recognized in the second derivative map. Band-structure calculations based on density functional theory (DFT) were carried out for the parent FeTe and are overlaid as solid lines in Fig. 1(a) after a suitable energy shift and rescaling which are ascribed to renormalization effects, as is known from earlier work[7,15–17]. The calculation details and complete band structure are discussed in the Supplementary Information and the energy shifts and rescaling are listed in Table 1. The calculated band

Table 1 | Energy shifts and rescaling values required for matching the calculated dispersions with the experimental dispersions	shift	scale
31 st	−130 meV	1/15
30 th	−278 meV	1/10
29 th	−110 meV	1/4.5
28 th	−110 meV	1/12

structure and orbital characters are also consistent with known results[24,25] and were confirmed by measuring the linear polarization dependence of spectral intensities (see Supplementary Information). However, in contrast to the DFT calculations which predict existence of three hole FSs around the Γ point, we find that the band top of the two dominantly *xz*/*yz*-orbital derived bands are located around 15 meV below E_F, i.e., these bands sink below E_F, and only one hole band originating in the x^2-y^2 orbital crosses E_F. From the degeneracy of the two *xz*/*yz* bands, we conclude that $k_z\sim 0$ in the reduced Brillouin zone for the present laser ARPES measurements.

The open circles in Fig. 1(a) show band dispersions deduced from the peak positions of the second derivative spectra shown in Fig. S3. The second derivative map after dividing by the FD function shown in Fig. S3(b) clearly shows that the dispersion around the Γ point is electron-like. The origin of this electronic dispersion is presumably another dominantly *xz*/*yz*-orbital derived band, which is located just above E_F for the DFT results for the parent FeTe (According to the reported DFT results for FeSe, the electronic disperion is located at ~0.5 eV above E_F at the Γ point. Hence, we can expect that the electron band in the DFT regime is located at ~0.2 eV above E_F for $FeTe_{0.6}Se_{0.4}$. This is small enough to be shifted just above EF by a renormalization effect, because the two hole bands which are predicted to make Fermi surfaces by the DFT calculations get shifted below E_F). For checking the dispersions above E_F, Fig. 1(b) shows the band dispersions in a narrow energy window near E_F, and band dispersions deduced from fits to the EDCs are overlaid. The fits to the EDCs, obtained after dividing by the FD function, are shown in Fig. 1(c). It is clear that there are two bands above E_F at the Γ-point, which get merged around $k\sim 0.07$ Å and then again separate out into two bands around $k\sim 0.1$ Å. Figure 1(d) shows the fits with the component Lorentzian functions for these three cases. We also performed measurements with another sample at higher temperatures of 35 K and 50 K in addition to 25 K as shown in Fig. S7. The peak positions are consistent with those shown in Fig. 1.

In the occupied states below E_F, the degenerate band top of the *xz*/*yz* hole bands are positioned at ~15 meV below E_F. The band top of the E_F-crossing x^2-y^2 band is located at least above ~6.5 meV from E_F at the Γ-point. Most interestingly, we do find the expected electron band existing just above E_F at the Γ-point, with the band bottom located at ~0.7 ± 0.2 meV above E_F (Fig. 1(b)). This electron band has been missed in all earlier studies of the momentum resolved electronic structure of Fe(Te,Se)[7,15–17]. We note that the x^2-y^2 hole band and the electron-like band just above E_F may be hybridized due to spin-orbit interactions (However, the spin-orbit interaction of Fe 3*d* states is ~70 meV, for Se 4*p* states is ~400 meV, and for Te 5*p* is ~1 eV[37], and all these values are significantly larger than the hole and electron-like dispersions being discussed here), for example, and result in a wing-shaped dispersion. However, even if these two bands are hybridized and merge to a single band, this does not affect our conclusions. Since the nature of the conducting carriers being electron-like or hole-like is determined by the gradient of the band dispersion ($\partial E/\partial k$), the carriers at k_F and the thermally-excited carriers at the Γ point will be hole-like and electron-like, respectively. Also, the details of electron band at the higher energy region above E_F are not relevant to superconductivity. Only the positions of the top of hole band and the bottom of the electron band are important, and they can be evaluated rather clearly from the MDCs, of which line shape is not affect by dividing by the FD function (see Supplementary Information).

Sharp superconducting coherence peak in the electron band just above E_F. Figures 2(a) and 2(b) show the energy distribution curves

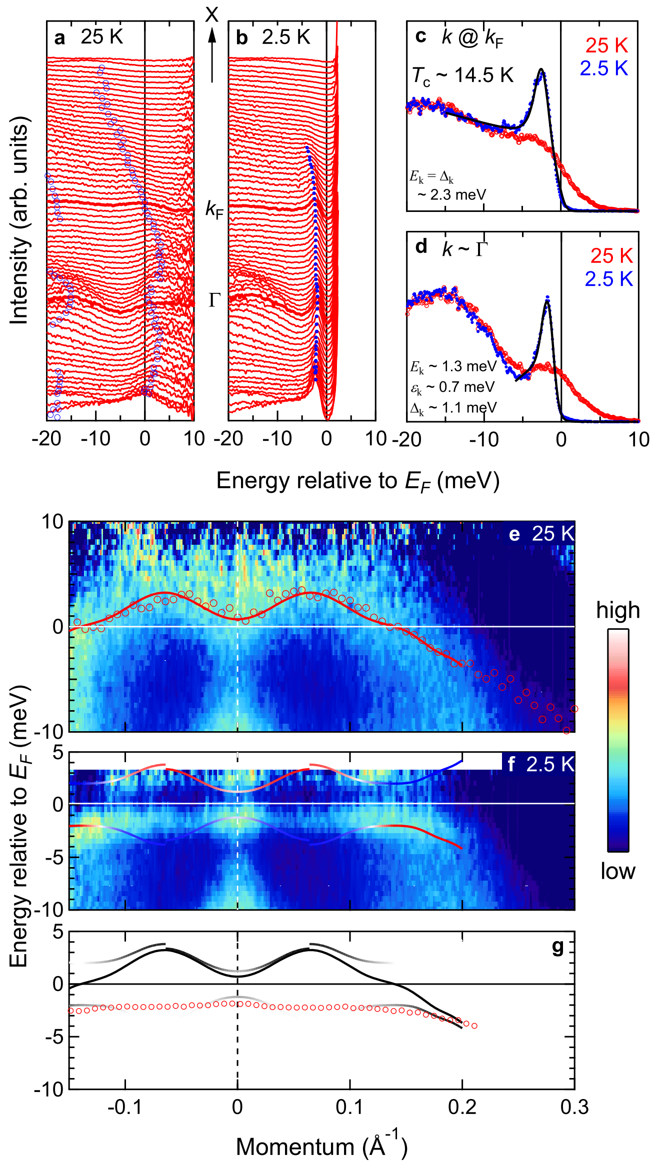

Figure 2 | Laser-ARPES spectra of $FeTe_{0.6}Se_{0.4}$ above and below T_c. FD-divided EDCs along Γ-*X* direction above T_c (a) and below T_c (b), respectively. EDCs above and below T_c at $k=k_F$ (c) and $k\sim\Gamma$ (d), respectively. The solid lines are the fitting results using the BCS spectral function. Intensity plots of the spectra above T_c (e) and below T_c (f), respectively. The solid line in panel (e) is a fitting result using a polynomial function for the dispersion indicated by the open circles. The solid lines in panel (f) are Bogoliubov quasiparticle (BQP) dispersions using the normal-state dispersion in panel (e) and the SC gap $\Delta(k)=2$ meV for the hole band and $\Delta(k)=1$ meV for the electron band, respectively. Colors of the lines correspond to the amplitude of coherence factors $|u_k|^2$ and $|v_k|^2$. The red and blue regions have larger and smaller coherence factors, respectively. (g) The normal-state and BQP dispersions have been plotted in the same panel. The open circles in panel (g) correspond to the dispersion of the coherence peaks at $T=2.5$ K in panel (b). The BQP dispersions merge for the electron and hole bands, indicative of a composite type of BCS-BEC superconductivity.

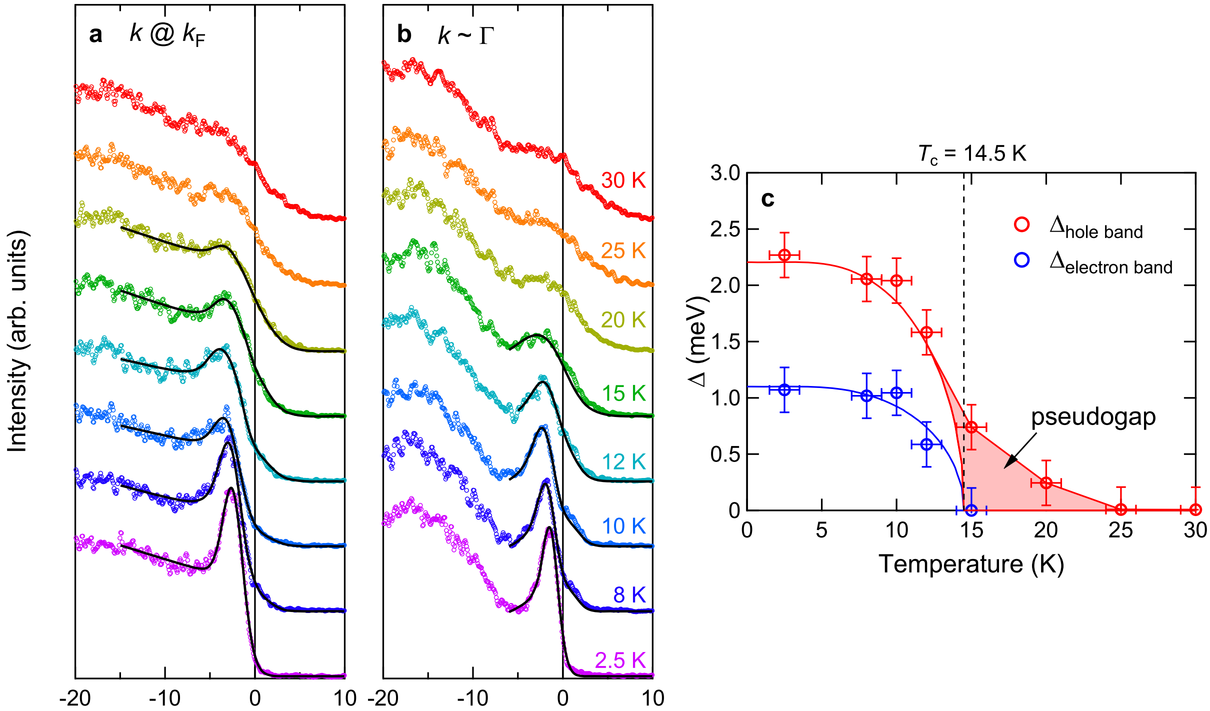

Figure 3 | Temperature dependence of EDCs at $k = k_F$ and $k \sim \Gamma$. Temperature dependence of raw EDCs at (a) $k = k_F$ of $x^2 - y^2$ hole-like band and (b) $k \sim \Gamma$ (bottom of the electron-like band), respectively. Fitting results with the BCS spectral function are indicated by black solid lines. (c), Temperature dependence of the obtained SC-gap sizes from the fitting to the BCS spectral function. Shaded area indicates pseudogap for the hole-like band.

(EDCs) after dividing by the FD functions corresponding to each temperature along Γ-X line at $T = 25$ K (above T_c) and at $T = 2.5$ K (below T_c), respectively. The open circles in Fig. 2(a) mark the normal-state band dispersions obtained from the second derivative spectra shown in Fig. S3. In Fig. 2(b), we can clearly see that the superconducting coherence peaks emerge below T_c for the hole band. The small circles in Fig. 2(b) mark the positions of the coherence peaks, and they are plotted in the enlarged scale in Fig. S10. Figures 2(c) and 2(d) show the EDCs above T_c (25 K) and below T_c (2.5 K) at $k = k_F$ and $k \sim \Gamma$, respectively. We can see that the electron band just above E_F at the Γ point also shows a sharp superconducting coherence peak, although this band does not cross the E_F in the normal state. The solid lines are fits to the BCS spectral function $A_{\mathrm{BCS}}(k, \omega)$[26–28], which can be expressed as

$$A_{\mathrm{BCS}}(k,\omega) = \frac{1}{\pi}\left\{\frac{|\mu_k|^2\Gamma}{(\omega - E_k)^2 + \Gamma^2} + \frac{|\nu_k|^2\Gamma}{(\omega + E_k)^2 + \Gamma^2}\right\},$$

where E_k and $|u_k|^2$, $|v_k|^2$ are the quasiparticle energy and the coherence factors of Bogoliubov quasiparticles (BQPs), respectively. Using the normal-state dispersion ϵ_k with respect to the chemical potential μ and the SC gap $\Delta(k)$, E_k can be expressed

$$E_k = \sqrt{(\epsilon_k - \mu)^2 + |\Delta(k)|^2}$$

and

$$|\mu_k|^2 = 1 - |\nu_k|^2 = \frac{1}{2}\left(1 + \frac{\epsilon_k}{E_k}\right),$$

respectively. From the fits to the data, we estimate the Bogoliubov quasiparticle energy $\left(E_k = \sqrt{\epsilon_k^2 + |\Delta(k)|^2}\right)$ of the hole band to be 2.3 meV ($=\Delta(k)$, because $\epsilon_k = 0$ at $k = k_F$ of this band) and of the electron band to be 1.3 meV, respectively. From the value of $\epsilon_k \sim 0.7$ meV, $\Delta(k)$ is estimated to be $\sim$1.1 meV for the electron band. This indicates different pairing strengths and reduced gap values $2\Delta/k_BT_c$ for the electron and hole bands. In addition, Δ/ϵ_F for the hole band is estimated to be $\sim$0.3, corresponding to a relatively weak coupling. On the other hand, since the energy position of the electron band is just 0.7 meV ($\sim$8 K) above E_F, it means that its occupancy in the normal state will strongly depend on temperature. Accordingly, the exact value of ϵ_F of the electron band cannot be described in the usual way. If we regard T_c as a measure of ϵ_F, based on the fact that T_c is the lowest temperature representing the normal state ($T_c = 14.5$ K $\sim$ 1.2 meV), we obtain $\Delta/\epsilon_F \geq 1$, indicative of the strong coupling limit. This estimation may seem to be fairly rough. However, if ϵ_F equals to Δ, the bottom of the electron band should be located at $E = -\Delta$ below E_F. Hence, we can say at least $\Delta/\epsilon_F \geq 1$. Thus, the electron band with a smaller Δ is actually in the strong-coupling regime. This represents the condition of an electron band with only a small number of carriers, but with a strong pairing interaction and a finite Δ exists for this band. On the otherhand, the hole band with a larger Δ lies in the relatively weaker-coupling regime. It is suggestive of Cooper pairing for the hole band and Boson condensation for the electron band. We note that even for the strong-coupling electron band, we have used a BCS spectral function to estimate the value of Δ. This is not a problem as the obtained value of Δ represent the lower bound of Δ, because a smaller value of ϵ_k-μ for the BEC regime will give a larger value of Δ[7,13].

Figures 2(e) and 2(f) show the intensity maps of the spectra above and below T_c, respectively, after dividing by the corresponding FD functions. The open circles are the same as in Fig. 2(a) and the solid line is a fitting result to the open circles using a polynomial function, representing the normal-state dispersion ϵ_k (Here, the normal state dispersions of the hole and electron bands merge to a single band. This means that these two bands are assumed to be hybridized at the band crossing). The solid lines in Fig. 2(f) are the BQP dispersions using ϵ_k in Fig. 2(e) and the Δ_k values obtained above for the electron and hole bands. Colors of the lines corresponds to the amplitude of the coherence factors $|u_k|^2$ above E_F and $|v_k|^2$ below E_F. The red and

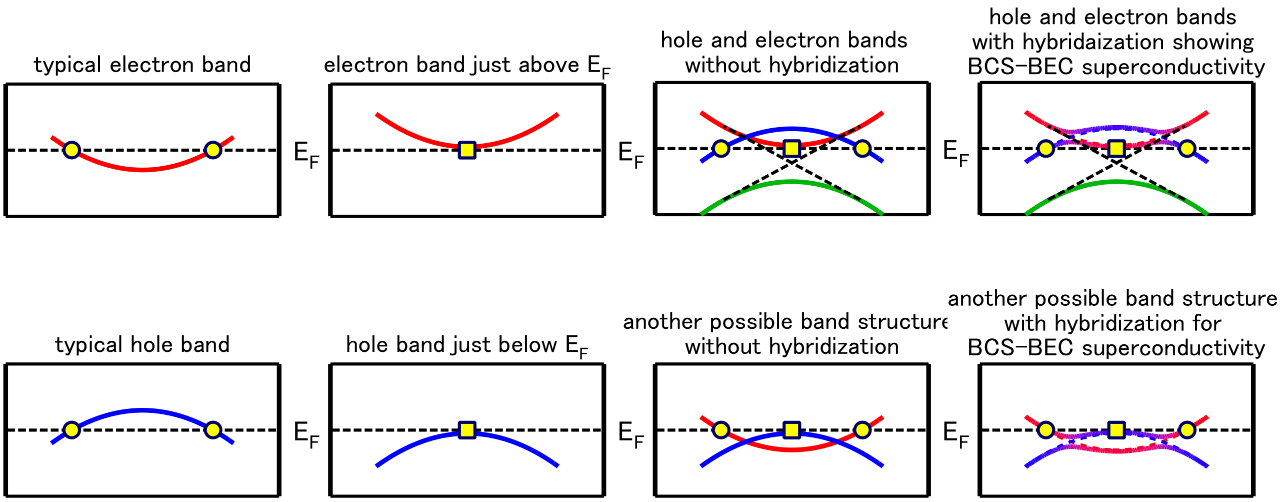

Figure 4 | Schematic band structure showing: a typical electron band, a typical hole band, an electron band lying just above E_F, the band structure in the absence of hybridization, and with hybridization showing composite BCS-BEC superconductivity. Similarly, a hole band lying just below E_F and another possible route to BCS-BEC superconductivity. The black dashed lines show similarity to Dirac point dispersion (see also Fig. S1 for relation with band-structure calculations).

blue regions correspond to the higher and lower values, respectively. It is noted that the BQP dispersion does not cross the brightest intensity around the Γ point above E_F. This is attributed to the tail of the hole-band top, which is also positioned at the Γ-point. The normal-state and BQP dispersions have been plotted in the same panel of Fig. 2(g). The open circles plotted in Fig. 2(g) correspond to the dispersion of the coherence peaks at $T = 2.5$ K shown in Fig. 2(b). The gray-scale density of the BQP dispersion corresponds to the amplitude of coherence factors. It is interesting to note that the BQP dispersions merge for the electron and hole bands, indicative of a composite BCS-BEC superconductivity. The results indicate that irrespective of weak or strong coupling, both the hole and electron bands in the superconducting state exhibit Bogoliubov quasiparticle dispersions due to particle-hole mixing[29]. However, the superconductivity in the electron band can be expected to be very sensitive to the occupancy of the electron band with Se substitution for Te, as well as pressure/strain. This possibly explains the reported large variation in T_c with pressure for FeSe ($T_c = 8.5$–36.7 K)[30].

Discussion

Another difference can be recognized between the weak-coupling hole band and the strong-coupling electron band. Figures 3(a) and 3(b) show the temperature dependence of EDCs at k_F for the hole band and $k \sim \Gamma$ for the electron band, respectively. The black solid lines indicate the fitting results using the BCS spectral function. The estimated SC-gap sizes are shown in Fig. 3(c). The existence of the pseudogap only for the hole band is clearer from the symmetrized EDCs (Fig. S11) or the FD-divided EDCs (Fig. S12). The temperature dependence of the gap opening indicates another important difference for the weaker-coupling hole band compared to the strong-coupling electron band. A pseudogap behavior can be recognized for the weaker coupling hole band in the spectra above T_c (The exsitence of the pseudogap for the hole band can be clearly recognized also from the temperature-dependent symmetrized EDC (see Fig. S9)). However, in strong contrast to the currently available BCS-BEC crossover theory[21] which predict existence of a pseudogap in the BEC strong coupling regime, the electron band does not show a pseudogap above T_c (This observation might lead to suspect that the superconducting gap near the Γ point is not originated from the electron band, but just a continuation from the BQP near k_F. However, as shown in Fig. S5, the observation of the superconducting coherence peaks well separately at $k = k_F$ and the Γ point evidently indicate that the superconducting gap at the Γ point is originated from the electron band just above E_F). Thus, we find a coexistence of the weak coupling and strong coupling superconductivity in the same material but with attributes not fully consistent with our present understanding of weak and strong coupling superconductivity. Our study identifies the required band structure for composite superconductivity, which is closely related to Dirac point dispersions, coexisting with a simple electron or hole band as schematically shown in Fig. 4.

Methods

Single crystals of $FeTe_{0.6}Se_{0.4}$ were prepared by a melt-growth technique. Chemical composition of the grown crystals was determined by electron probe microanalysis (EPMA) and inductively coupled plasma (ICP) atomic emission spectrometry. Details have been described in Ref. 31. ARPES data were collected using the laser ARPES apparatus developed at ISSP with the 6.994 eV, 6th harmonic of $Nd:YVO_4$ quasi continuous wave (q-CW, repetition rate = 120 MHz) laser and VG-Scienta HR8000 electron analyzer[28]. While this apparatus achieves the maximum energy resolution of 70 μeV, the overall energy resolution was set to $\sim$1.2 meV for the measurements of EDCs and MDCs near E_F and 5 meV for E-k map measurements, The angular resolution was 0.1 deg, corresponding to the momentum resolution of 0.0015 Å^{-1}. Polarization of incident excitation laser was adjusted using a half-wave (λ/2) plate and a quarter-wave (λ/4) plate. The E_F positions were calibrated by measuring the Fermi edge of a gold film evaporated onto the sample substrate.

1. Kamihara, Y., Watanabe, T., Hirano, M. & Hosono, H. Iron-Based Layered Superconductor $La[O_{1-x}F_x]FeAs$ (x = 0.05–0.12) with T_c = 26 K. *J. Am. Chem. Soc* **130**, 3296–3297 (2008).
2. Mazin, I. I., Singh, D. J., Johannes, M. D. & Du, M. H. Unconventional Superconductivity with a Sign Reversal in the Order Parameter of $LaFeAsO_{1-x}F_x$. *Phys. Rev. Lett.* **101**, 057003 (2008).
3. Kuroki, K. *et al.* Unconventional Pairing Originating from the Disconnected Fermi Surfaces of Superconducting $LaFeAsO_{1-x}F_x$. *Phys. Rev. Lett.* **101**, 087004 (2008).
4. Kontani, H. & Onari, S. Orbital-Fluctuation-Mediated Superconductivity in Iron Pnictides: Analysis of the Five-Orbital Hubbard-Holstein Model. *Phys. Rev. Lett.* **104**, 157001 (2010).
5. Lu, D. H. *et al.* Electronic structure of the iron-based superconductor LaOFeP. *Nature* **455**, 81–84 (2008).
6. Zabolotnyy, V. B. *et al.* (π, π) electronic order in iron arsenide superconductors. *Nature* **457**, 569–572 (2009).
7. Lubashevsky, Y., Lahoud, E., Chashka, K., Podolsky, D. & Kanigel, A. Shallow pockets and very strong coupling superconductivity in $FeSe_xTe_{1-x}$. *Nat. Phys.* **8**, 309–312 (2012).
8. Ding, H. *et al.* Spectroscopic evidence for a pseudogap in the normal state of underdoped high-Tc superconductors. *Nature* **382**, 51–54 (1996).
9. Loeser, A. G. o. Excitation Gap in the Normal State of Underdoped $Bi_2Sr_2CaCu_2O_{8+\Delta}$. *Science* **273**, 325–329 (1996).

10. Lee, W. S. *et al.* Abrupt onset of a second energy gap at the superconducting transition of underdoped Bi2212. *Nature* **450**, 81–84 (2007).
11. Yang, H.-B. *et al.* Emergence of preformed Cooper pairs from the doped Mott insulating state in $Bi_2Sr_2CaCu_2O_{8+\Delta}$. *Nature* **456**, 77–80 (2008).
12. Kondo, T., Khasanov, R., Takeuchi, T., Schmalian, J. & Kaminski, A. Competition between the pseudogap and super-conductivity in the high-Tc copper oxides. *Nature* **457**, 296–300 (2009).
13. Gaebler, J. P. *et al.* Observation of pseudogap behaviour in a strongly interacting Fermi gas. *Nat Phys* **6**, 569–573 (2010).
14. Chen, Q., Stajic, J., Tan, S. & Levin, K. BCS-BEC crossover: From high temperature superconductors to ultracold superfluids. *Physics Reports* **412**, 1–88 (2005).
15. Chen, F. *et al.* Electronic structure of $Fe_{1.04}Te_{0.66}Se_{0.34}$. *Phys. Rev. B* **81**, 014526 (2010).
16. Tamai, A. *et al.* Strong Electron Correlations in the Normal State of the Iron-Based $FeSe_{0.42}Te_{0.58}$ Superconductor Observed by Angle-Resolved Photoemission Spectroscopy. *Phys. Rev. Lett.* **104**, 097002 (2010).
17. Nakayama, K. *et al.* Angle-Resolved Photoemission Spectroscopy of the Iron-Chalcogenide Superconductor $Fe_{1.03}Te_{0.7}Se_{0.3}$: Strong Coupling Behavior and the Universality of Interband Scattering. *Phys. Rev. Lett.* **105**, 197001 (2010).
18. Eagles, D. M. Possible Pairing without Superconductivity at Low Carrier Concentrations in Bulk and Thin-Film Superconducting Semiconductors. *Phys. Rev.* **186**, 456–463 (1969).
19. Leggett, A. *Modern trends in the theory of condensed matter.* Springer-Verlag, Berlin, (1980).
20. Randeria, M., Duan, J.-M. & Shieh, L.-Y. Bound states, Cooper pairing, and Bose condensation in two dimensions. *Phys. Rev. Lett.* **62**, 981–984 (1989).
21. Sá de Melo, C. A. R., Randeria, M. & Engelbrecht, J. R. Crossover from BCS to Bose superconductivity: Transition temperature and time-dependent Ginzburg-Landau theory. *Phys. Rev. Lett.* **71**, 3202–3205 (1993).
22. Timmermans, E., Furuya, K., Milonni, P. W. & Kerman, A. K. Prospect of creating a composite Fermi-Bose superfluid. *Physics Letters A* **285**, 228–233 (2001).
23. Regal, C. A., Greiner, M. & Jin, D. S. Observation of Resonance Condensation of Fermionic Atom Pairs. *Phys. Rev. Lett.* **92**, 040403 (2004).
24. Subedi, A., Zhang, L., Singh, D. J. & Du, M. H. Density functional study of FeS, FeSe, and FeTe: Electronic structure, magnetism, phonons, and superconductivity. *Phys. Rev. B* **78**, 134514 (2008).
25. Miyake, T., Nakamura, K., Arita, R. & Imada, M. Comparison of *Ab initio* Low-Energy Models for LaFePO, LaFeAsO, $BaFe_2As_2$, LiFeAs, FeSe, and FeTe: Electron Correlation and Covalency. *J. Phys. Soc. Jpn* **79**, 044705 (2010).
26. Matsui, H. *et al.* BCS-Like Bogoliubov Quasiparticles in High-T_c Superconductors Observed by Angle-Resolved Photoemission Spectroscopy. *Phys. Rev. Lett.* **90**, 217002 (2003).
27. Shimojima, T. *et al.* Orbital-Independent Superconducting Gaps in Iron-Pnictides. *Science* **332**, 564 (2011).
28. Okazaki, K. *et al.* Octet-Line Node Structure of Superconducting Order Parameter in KFe_2As_2. *Science* **337**, 1314–1317 (2012).
29. Campuzano, J. C. *et al.* Direct observation of particle-hole mixing in the superconducting state by angle-resolved photoemission. *Phys. Rev. B* **53**, R14737–R14740 (1996).
30. Medvedev, S. *et al.* Electronic and magnetic phase diagram of β-$Fe_{1.01}Se$ with superconductivity at 36.7 K under pressure. *Nature Mater* **8**, 630–633 (2009).
31. Hanaguri, T., Niitaka, S., Kuroki, K. & Takagi, H. Unconventional *s*-Wave Superconductivity in Fe(Se, Te). *Science* **328**, 474–476 (2010).
32. Herman, F. & Skillman, S. *Atomic structure calculations.* Prentice-Hall, New Jersey, (1963).

Acknowledgments

We would like to thank K. Kuroki and R. Arita for valuable discussions and comments. This research is supported by JSPS through its FIRST Program.

Author contributions

K.O., Y.O., Y.K., T.S. and T.K. developed the laser-ARPES apparatus; S.W. and C.T.C. developed the 7-eV laser system using the nonlinear optical crystal; S.N., T.H. and H.T. grew high-quality single crystals and characterized them; K.O., Y.I. and Y.O. performed the experiments and data analysis; K.O. and A.C. wrote the manuscript; S.S. designed the project; All authors discussed the results and commented on the manuscript.

Additional information

Supplementary information accompanies this paper at http://www.nature.com/scientificreports

Competing financial interests: The authors declare no competing financial interests.

How to cite this article: Okazaki, K. *et al.* Superconductivity in an electron band just above the Fermi level: possible route to BCS-BEC superconductivity. *Sci. Rep.* **4**, 4109; DOI:10.1038/srep04109 (2014).